Original Article

Impact of different cross-section designs of rotary instruments on smear layer removal, cyclic and torsional fatigue resistance: *In vitro* study

João Pedro Tadano, Murilo Priori Alcalde, Ana Grasiela Limoeiro, Raimundo Sales Oliveira-Neto, Paula Tereza Galvão[1], Guilherme Ferreira da Silva, Pablo Amoroso-Silva[2], Marco Antônio Duarte, Rodrigo Ricci Vivan

Department of Dentistry, Endodontics and Dental Materials, Bauru Dental School, University of São Paulo, SP, [1]Department of Endodontics, University Center of Grande Dourados, Dourados, MS, [2]Department of Endodontics, Universidade Estadual State University of Londrina, Londrina, PR, Brazil

Abstract

Introduction: In endodontics, mechanized nickel–titanium (NiTi) instruments are widely adopted for both initial treatments and retreatment because of their flexibility and minimal impact on root canal trajectory. This study aimed to assess the effect of four rotary NiTi systems on the quantity of smear layer remaining on dentin walls after instrumentation and to compare their resistance to cyclic and torsional fatigue.

Materials and Methods: Forty mandibular incisors ($n = 10$) were divided into four groups according to the file used for instrumentation: spin, S2, rotate, and platinum V.EU rotary files. Dentin wall evaluation for smear layer was performed through scanning electron microscopy. For mechanical tests, 80 instruments were used in total, with 40 instruments ($n = 10$ per group) undergoing cyclic fatigue analysis using an artificial canal apparatus and another 40 instruments ($n = 10$ per group) undergoing torsional fatigue analysis using a custom-designed torsion machine. All instruments had a 0.25 mm diameter and underwent cyclic and torsional fatigue analysis. Statistical analysis was conducted at a 5% significance level.

Results: Intergroup comparisons showed a comparable percentage of smear layer on dentin walls ($P > 0.05$). Cyclic fatigue tests indicated that spin and S2 instruments possessed the highest resistance ($P < 0.05$). The rotate system demonstrated the greatest angular deflection and the lowest torque ($P < 0.05$).

Conclusion: All tested rotary systems yielded similar smear layer accumulation but exhibited varying cyclic and torsional properties.

Keywords: Cyclic fatigue, endodontics, nickel–titanium instruments, root canal preparation, smear layer

Address for correspondence: Prof. Ana Grasiela Limoeiro, Rua Siqueira Campos, 180, Centro, Vitória Da Conquista, Bahia, 45000-455, Brazil.
E-mail: grasielalimoeiro@gmail.com
Submission: 18-07-25 **Revision:** 28-08-25 **Acceptance:** 02-09-25 **Web Publication:** 30-12-25

INTRODUCTION

Mechanized nickel–titanium (NiTi) instruments are widely utilized in endodontic procedures, including initial treatments and retreatment, primarily due to their flexibility and minimal tendency to create deviations in the root canal trajectory.[1] However, navigating highly constricted (atresic)

Access this article online	
Quick Response Code:	Website: www.saudiendodj.com
	DOI: 10.4103/sej.sej_160_25

How to cite this article: Tadano JP, Alcalde MP, Limoeiro AG, Oliveira-Neto RS, Galvão PT, da Silva GF, *et al*. Impact of different cross-section designs of rotary instruments on smear layer removal, cyclic and torsional fatigue resistance: *In vitro* study. Saudi Endod J 2026;16:106-14.

root canals increases the risk of the instrument tip binding against dentinal walls, potentially leading to torsional deformation or fracture.[2] Therefore, manufacturers have developed various systems incorporating diverse heat treatments and cross-sectional geometries to enhance the mechanical properties and safety of these instruments when shaping canals with complex anatomy.[3]

Numerous novel NiTi instrument systems featuring unique designs and thermal modifications have been introduced, aiming to optimize their mechanical characteristics, shaping efficiency, and efficacy in removing root canal debris.[4] Specific features of instrument design, such as their cross-sectional geometry, the depth of their helical flutes, core diameter, and the cutting blade's helical angle, directly influence how debris is generated and subsequently cleared during root canal instrumentation.[4,5] For instance, the S-shaped cross-section has become prevalent due to its advantageous mechanical properties[6] and its contribution to effective debris removal.[5]

Instruments featuring a "flat surface design," which originate from S-shaped cross-sections refined through an additional machining step, are engineered to reduce the screwing effect, increase flexibility, and enhance debris evacuation by omitting conventional cutting blades.[4]

An example is the S2 system, which incorporates an asymmetric S-section where one side of the cutting blades is less prominent. According to the manufacturer, this design feature aims to decrease wall friction and facilitate more efficient root canal debris removal. Nevertheless, current literature lacks empirical evidence validating whether this specific cross-section delivers the advantages claimed by its manufacturer.

Acknowledging the necessity for further investigation into the influence of flat and asymmetric S-sections on debris clearance within the root canal, the present study sought to compare the quantity of smear layer remaining on dentin walls after instrumentation with files possessing conventional S, asymmetric S, and flat cross-sectional designs. Furthermore, the study assessed the cyclic and torsional fatigue resistance of these instruments.

The null hypotheses formulated for this investigation were as follows: (i) no significant difference would be observed in the presence of smear layer on root canal walls among the tested instrument groups; and (ii) no significant difference would be found in the cyclic and torsional fatigue resistance of the instruments.

MATERIALS AND METHODS

This laboratory investigation adhered to the PRILE 2021 guidelines [Figure 1][7] and received approval from the Human Research Ethics Committee (CAAE 28293620.6.3001.5417), adhering to the Helsinki Declaration's ethical standards.

For the study, 120 mandibular incisors underwent initial radiographic evaluation to assess their root canal anatomy in both buccolingual and mesiodistal planes. This imaging was conducted using a digital sensor (Fona CDR Elite; DMM Health, Bandeirantes, PR, Brazil). Teeth were deemed suitable for inclusion if their buccolingual diameter measured twice that of their mesiodistal diameter. Furthermore, only incisors exhibiting Vertucci type I canals and no history of previous endodontic treatment, were selected. Teeth that did not meet these inclusion criteria or exhibited signs of root resorption, calcification, or open apices were excluded from the study.

Group definitions

The study utilized four different rotary NiTi systems, each characterized by its cross-sectional design: the Spin Rotary system (MK Life, Porto Alegre, RS, Brazil) with a conventional S-shaped cross-section; the S2 system (Bassi/Easy Equipamentos Odontológicos, Belo Horizonte, MG, Brazil) with an asymmetric S-shaped cross-section; the Rotate system (Dentsply/Maillefer, Ballaigues, Switzerland) with a conventional S-shaped cross-section; and the Platinum V.EU system (Bondent Group, Changzhou, China) with a flat cross-section.

Smear layer evaluation by scanning electron microscopy

To evaluate the presence of smear layer on dentin walls, 40 mandibular incisors were used. Sample size calculation was performed using the Chi-square test and variance statistics (G*Power v3.1 for Mac [Heinrich Heine, University of Düsseldorf, Germany]), with alpha error of 0.05 and beta power of 0.95, and indicated that a minimum of 10 specimens per group was necessary, corroborating a previous study.[8]

All procedures described below were performed under an operating microscope (DFVasconcellos, Valença, RJ, Brazil) by the same operator, an experienced endodontist with more than 10 years of clinical experience. Access opening was performed using diamond burs under water cooling. A K-10 instrument (Dentsply, Ballaigues, Switzerland) was introduced until its tip was visible in the apical foramen, and the working length was adjusted by reducing 1 mm from this measurement. All measurements were noted, and the teeth were enumerated and randomly (https://www.random.org/) divided according to the system to be

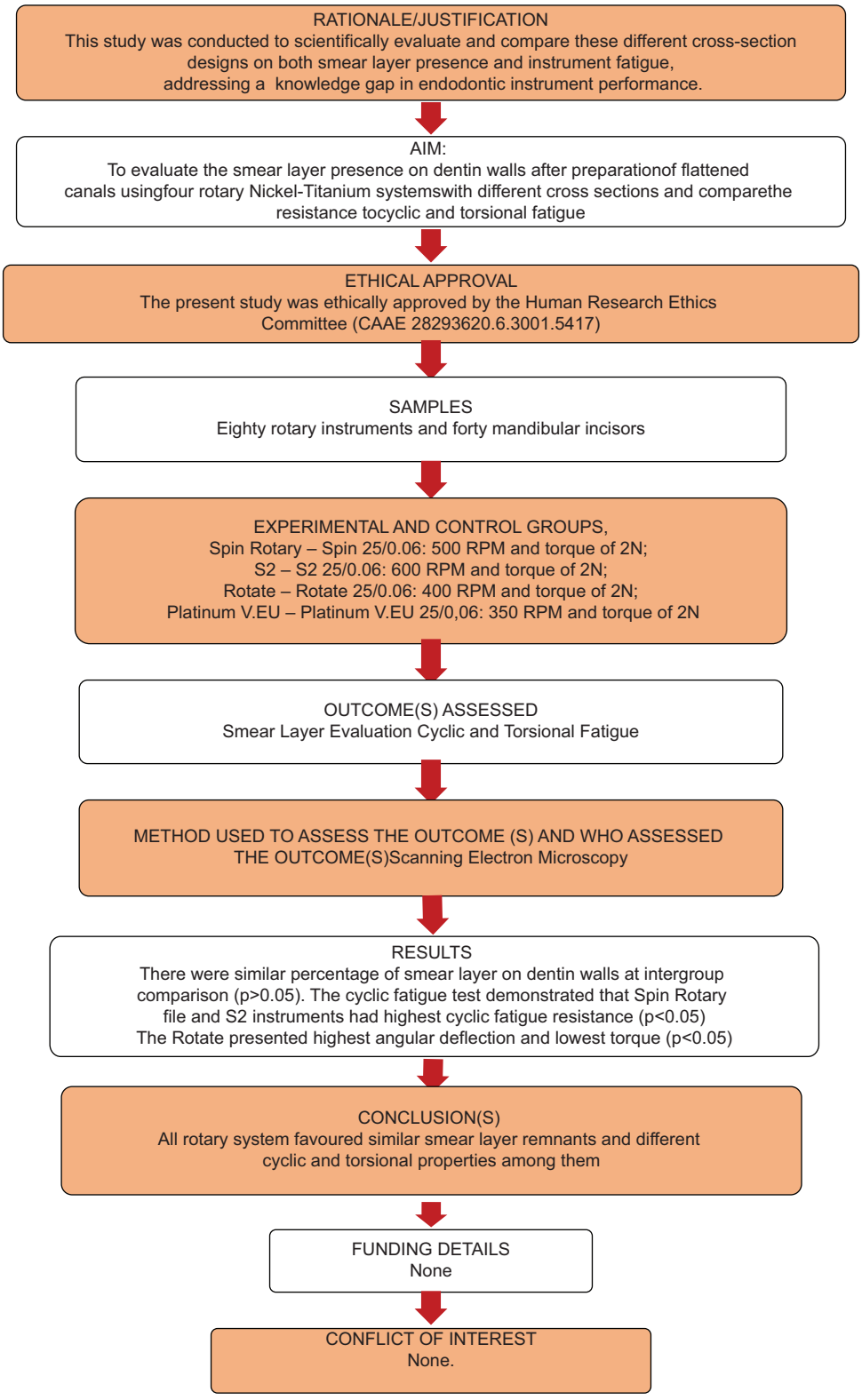

Figure 1: PRILLE flowchart

instrumented (n = 10). The instruments were driven by a VDW Silver electric endodontic motor (VDW, Munich, Germany) configured with speed and torque according to the manufacturer's recommendations [Table 1].

Each instrument was used to instrument five specimens before replacement. Between each instrument, 5 mL of 2.5% sodium hypochlorite (NaOCl) was irrigated using a 30G needle inserted 1 mm short of the WL, at a flow rate

Table 1: Rotary files speed and torque used during root canal preparation

System	Coronal Flaring	Glide Path	Working length
Spin	17.08 – 350 RPM and 1.5 N.cm	15.04 – 350 RPM and 1.5 N.cm	20.05, 25.06 and 35.04 – 500 RPM and 2 N.cm
S2	15.10 – 350 RPM and 2 N.cm	15.05 – 350 RPM and 2 N.cm	25.06 and 35.04 – 600 RPM and 2 N.cm
Rotate	-	15.04 – 350 RPM and 1.3 N.cm	20.05, 25.06 and 35.04 – 400 RPM and 2 N.cm
Platinum	17.12 – 300 RPM and 1.5 N.cm	15.04 – 350 RPM and 2.4 N.cm	25.04 and 30.04 – 350 RPM and 2.0 N.cm

RPM: Revolutions per minute

of 0.5 mL per second. In total, 20 mL of 2.5% NaOCl was utilized for all samples and experimental groups.

Following instrumentation, all teeth were cleaved in the buccolingual direction using double-sided diamond discs (0.17 mm thickness and 22 mm diameter). This process involved creating canals on both the buccal and lingual surfaces, which was accomplished solely using a periotome. This approach ensured no debris formation in the canal, which could potentially interfere with subsequent analysis.

The mesial and distal hemisections were examined using environmental scanning electron microscopy (SEM) (Aspex Express; Fei Europe, Eindhoven, Netherlands) at ×500, with 20 kV beam energy, filament drive set at 62.5%, and an emission current of 47.2 μA. Images of the apical and middle third of each hemisection were captured, totaling 40 images per group, saved in tagged image file format (TIFF) format, and imported into Microsoft PowerPoint software (Microsoft Corporation, Redmond, USA).

To quantify the percentage of areas with smear layer on the dentin walls, the hemisection images were divided into 100 squares using a digital grid; each square represented an area of 27.5 μm^2 × 27.5 μm^2. The presence of the smear layer was evaluated by determining the number of squares within the grid that were devoid of visible dentinal tubules, which indicates the presence of the smear layer. Conversely, squares where dentinal tubules were clearly visible were considered "smear layer free" or "clean." The percentage of clean areas was calculated by dividing the number of clean squares by the total number of squares (100) and multiplying by 100. This analysis was performed at both the apical and middle thirds. Two independent examiners, previously calibrated and blinded to the study, evaluated the images.

Cyclic and torsional fatigue

For the mechanical tests, 80 NiTi rotary instruments, each measuring 25 mm in length, were employed. Sample size calculation was performed using G*Power version 3.1 for Mac (Heinrich Heine) with the Wilcoxon Mann–Whitney test for an alpha error of 0.05, beta power of 0.95, and N2/NI ratio of 1. To ensure robust statistical analysis, eight instruments per group were used. However, to account for potential outliers that could result in sample loss, an additional 20% of instruments were included. Thus, 10 instruments from each system were selected per test.

The cyclic fatigue test was conducted at room temperature (20°C) in an artificial stainless-steel canal featuring a 60° angle of curvature and a 5 mm radius, located 5 mm from the instrument's tip. The device enabled precise and reproducible positioning of the curvature for all instruments. This methodology has been previously described.[9] A total of 40 instruments were used, 10 per group, attached to the VDW Silver motor connected to the cyclic fatigue device. The instruments were activated as mentioned earlier, following the manufacturers' recommendations:

1. Spin system (25/0.06): 500 RPM and torque of 2N;
2. S2 system (25/0.06): 600 RPM and torque of 2N;
3. Rotate system (25/0.06): 400 RPM and torque of 2N;
4. Platinum system (25/0.06): 350 RPM and torque of 2N.

Before the test, the artificial canal was lubricated with synthetic oil (Super Oil; Singer Co. Ltd., Elizabethport, NJ, USA) to minimize instrument friction and prevent overheating resulting from friction. Fracture time was recorded using a digital stopwatch, and simultaneous video recording was conducted to ensure the accurate recording of the instrument's fracture time. In addition, the number of cycles to failure (NCF) was calculated by multiplying RPM by time (in seconds) divided by 60.

To assess torque and maximum angular deflection to fracture using the torsional fatigue test, 40 rotary system instruments were used (n = 10). Torsional tests were performed in accordance with the International Organization for Standardization 3630-1:1992, employing a torsion machine as previously described.[10] Maximum torque and angular deflection were measured using a custom-designed machine (Analógica, Belo Horizonte, MG, Brazil) connected to a computer. Data acquisition was facilitated through the machine's dedicated software (MicroTorque; Analógica).

Before commencing the test, instrument mandrels were removed at the point of fixation to the torsion axis. Subsequently, the 3 mm of instrument tips were fixed

in a mandrel connected to a geared motor operating in a clockwise direction, with a regulated speed of 2 RPM across all experimental groups.

Scanning electron microscopy evaluation after cyclic and torsional fatigue

Following the cyclic and torsional fatigue tests, 80 fractured instruments (n = 10 per group) were selected for SEM evaluation (JEOL; JSM-TLLOA, Tokyo, Japan) to examine the topographic features of the fragments. All instruments underwent cleaning in an ultrasonic device (Gnatus, Ribeirão Preto, SP, Brazil) using distilled water for 3 min postmechanical testing as per previous protocols.[9,11,12] Fractured instrument surfaces were examined under ×250 after the cyclic fatigue test. In addition, the fractured surfaces of instruments subjected to torsional testing were assessed under ×250 and ×1000, focusing on the center of the surface.

Statistical analysis

All statistical tests were performed using the GraphPad Prism 9.0 (GraphPad Software Inc., La Jolla, CA, USA) with a significance level of 5%.

Smear layer evaluation

The kappa tests showed a high level of agreement between the two examiners (0.85). Data were first analyzed for normality using the Kolmogorov–Smirnov test. As a normal distribution was not observed for the wall cleaning test, data were compared using the Kruskal–Wallis and Dunn test.

Cyclic and torsional fatigue

Data were statistically analyzed for normality using the Kolmogorov–Smirnov test. As a normal distribution was observed, the analysis of variance and Tukey tests were employed.

RESULTS

The median, minimum, and maximum values of smear layer-free walls (in percentage) are presented in Table 2. Representative SEM images of the study groups are depicted in Figure 2. Intergroup analysis demonstrated no significant difference in the percentage of smear layer-free walls ($P > 0.05$). In addition, intragroup analysis demonstrated no significant difference between the middle and apical thirds ($P > 0.05$).

Table 3 describes the means and standard deviations of the cyclic fatigue tests (maximum time and NCF and torsional fatigue (maximum torque load and angle of rotation). The results of the cyclic fatigue test revealed that the platinum V.EU 25.06 exhibited a significantly longer time to fracture than the other groups ($P < 0.05$). The spin rotary 25.06 and

Table 2: Median, minimum and maximum values (in percentage %) of root canal walls free of smear layer evaluated by Scanning Electron Microscopy

Instruments	Middle	Apical
Spin 25.06	32.5 (5-99)^{a,A}	2 (0-96)^{a,B}
S2 25.06	25.5 (2-99)^{a,A}	1.5 (0-87)^{a,B}
Platinum 25.06	25.6 (1-100)^{a,A}	3.5 (0-65)^{a,B}
Rotate 25.06	58.5 (6-95)^{a,A}	6 (2-90)^{a,B}

Equal superscript lowercase letters in the same column means no significant intergroup differences in the percentage of smear layer-free walls and equal superscript uppercase letters in the same column means no significant intragroup difference between the middle and apical thirds ($P>0.05$)

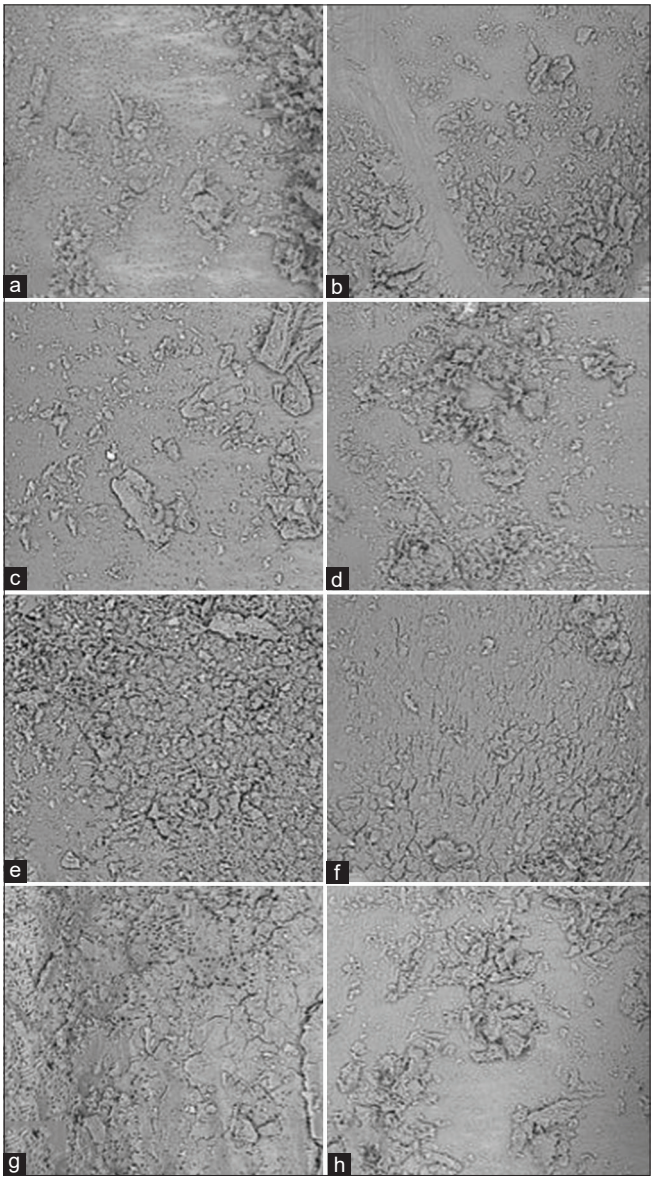

Figure 2: Representative scanning electron microscopy images of the middle and apical thirds of evaluated groups after instrumentation. (a and b) the middle and apical thirds of the spin group; (c and d) the middle and apical thirds of the S2 group; (e and f) the middle and apical thirds of the platinum V.EU group; (g and h) the middle and apical thirds of the rotate group

S2 25.06 instruments showed no significant difference in fracture time ($P > 0.05$), while the rotate 25.06 instrument showed the shortest time to fracture ($P < 0.05$). Regarding NCF, the spin rotary 25.06 and S2 25.06 instruments exhibited significantly higher values than the platinum V.EU 25.06 and rotate 25.06 instruments ($P < 0.05$). The rotate 25.06 instrument presented the lowest NCF among the groups ($P < 0.05$).

In the torsional fatigue test, a significant difference was observed in torque only in the rotate 25.06 instrument group compared to the other groups ($P < 0.05$). Conversely, the rotate 25.06 instrument exhibited greater angular deflection than the other groups ($P < 0.05$). There were no significant differences in torque or angular deflection between S2 25.06, spin rotary 25.06, and platinum V.EU 25.06 instruments ($P > 0.05$).

Following cyclic fatigue, numerous dimples were observed on the fractured surface [Figure 3]. After the torsion test, the fragments exhibited typical characteristics of shear rupture, showing concentric abrasion marks and microscopic fibrous dimples [Figure 4].

DISCUSSION

This study addressed two key questions: the influence of different cross-sectional designs on smear layer remaining on dentin walls after instrumentation with files possessing different cross-sectional designs, in addition to assessing their cyclic and torsional fatigue resistance. These questions are critical for improving safety and effectiveness during biomechanical preparation of root canals, as initially highlighted in the introduction.

The flat section design was introduced to enhance flexibility, improve cyclic fatigue resistance, and facilitate root canal debris removal.[4,13]

Preparing flattened canals presents specific challenges due to an increased propensity for debris impaction and difficulties in thoroughly cleaning these root canal systems, particularly in the apical third.[14] For this reason, mandibular incisors were used in this study to assess the presence of the smear layer. Although microcomputed tomography (Micro-CT) is extensively employed for assessing debris within the root canal system, SEM remains the preferred method for assessing and quantifying smear layer on dentin[15] since micro-CT lacks the resolution to analyze smear layer, which typically measures between 1 and 2 μm in dimension.[16]

All instruments generate dentin debris during instrumentation, particularly in the apical third.[17,18] This phenomenon may be attributed to cutting capacity and design characteristics such as cross-section, helical canal, and cutting blade angle. Our findings corroborate these previous observations, as all systems, regardless of cross-sectional design, exhibited a similar extent of debris-free canal walls across the evaluated thirds. Therefore, the first null hypothesis was accepted.

Despite no difference in the percentage of debris-free walls in intergroup analysis, the results for the rotate system indicated a tendency toward more effective smear layer removal in the evaluated thirds, even when compared to the spin rotary system, which shares a similar cross-sectional design. In addition, there was a slight tendency toward fewer smear layer-free walls in the groups with flat and asymmetric S-shaped sections, although without statistical significance. Hence, it can be speculated that the symmetric S-shaped section exhibited a tendency toward smear layer removal. However, this was not significantly different in our study, which aligns with previous findings.[4,18]

Despite not having a significant difference, all rotary systems exhibited smaller amounts of walls without debris in the apical third than in the middle third in the intragroup analysis, corroborating previous studies.[18,19] A primary factor contributing to this reduced cleaning efficiency in the apical region is attributed to reduced irrigation effectiveness in this area.[8,18] In addition, characteristics such as depth of the helical canal, cutting blade angle, and number of cutting blades can influence efficiency.[18,19] This is further evident when comparing instruments with the same cross-section (rotate and spin rotary system), where rotate exhibited a greater cleaning tendency, although without a significant difference. Therefore, the varying design characteristics (cross-section,

Table 3: Mean and Standard Deviation of cyclic fatigue (time in seconds and number of cycles until fracture) and Torsional fatigue (torque and angular deflection)

Instruments	Cyclic Fatigue		Torsional Fatigue	
	Time (s)	NCF	Torque (N.cm)	Angular Deflection (°)
Spin 25.06	253.4±17.58^{a}	2238±155.3^{a}	1.18±0,09^{a}	396.6±11.77^{a}
S2 25.06	229.7±15.1^{a}	2297±150.0^{a}	1.23±0,13^{a}	393.8±14.70^{a}
Rotate 25.06	203.8±15.39^{b}	1188±90.92^{b}	0.85±0,09^{b}	453.1±27.11^{b}
Platinum 25.06	295.8±48.43^{c}	1725±283.6^{c}	1.15±0,12^{a}	391.7±20.58^{a}

Different superscript lowercase in the same column means significant intergroup differences ($P<0.05$). NCF: number of cycles until fracture

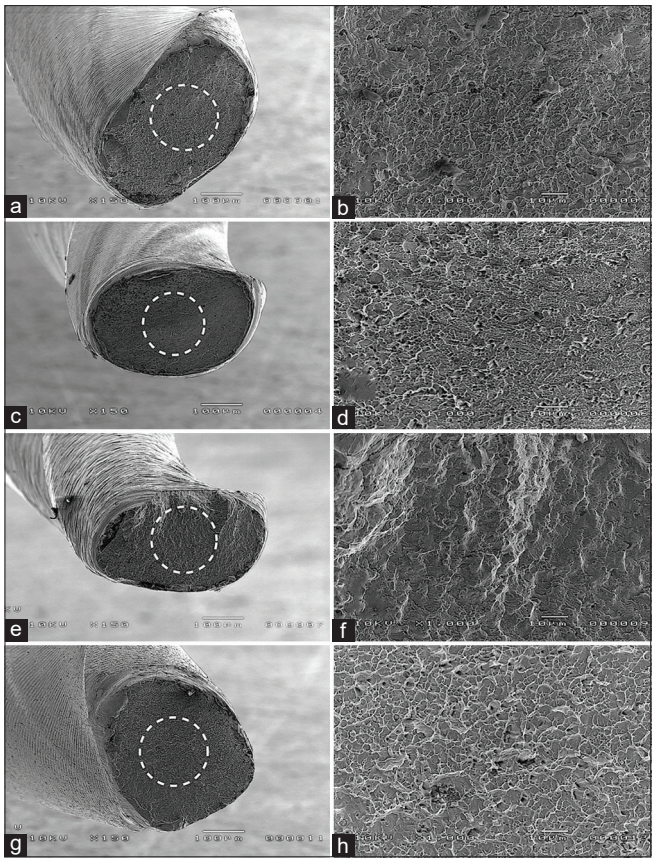

Figure 3: Scanning electron microscopy images of the fractured surfaces of separate fragments after cyclic fatigue test; first row: (a and b) VDW rotate 25.06; second row: (c and d) spin rotary file 25.06; third row: (e and f) S2 25.06; fourth row: (g and h) platinum V.EU 25.06. The left column shows the images with numerous dimples spread on the fractured surfaces, which constitute a typical feature of ductile fracture at ×150; the right column shows the dimples on the fractured surface at ×1000

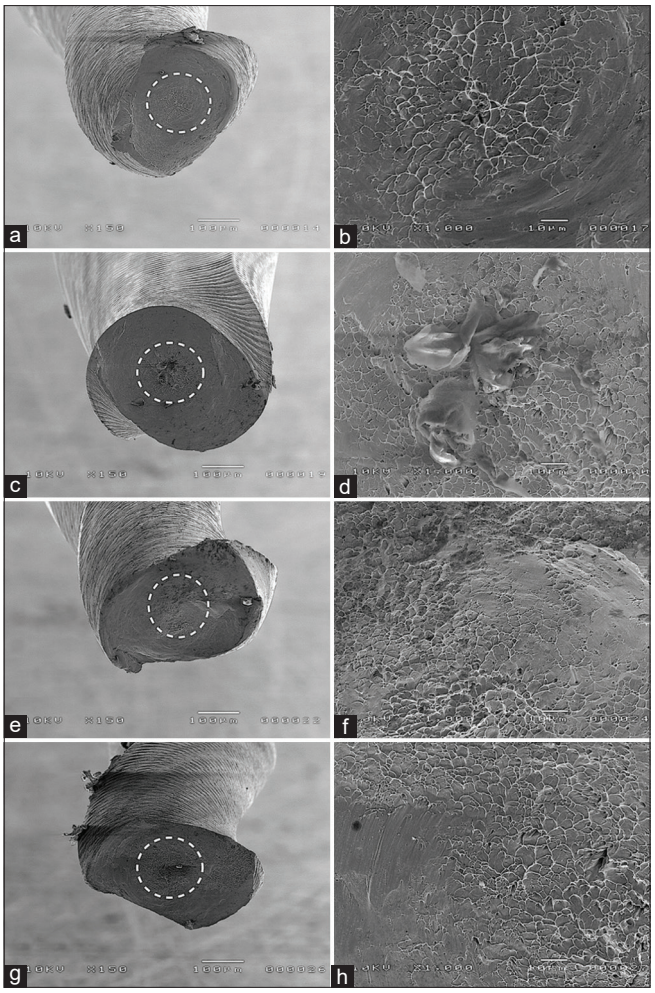

Figure 4: Scanning electron microscopy images of the fractured surfaces of separate fragments after cyclic fatigue test, first row: (a and b) VDW rotate 25.06; second row: (c and d) spin rotary file 25.06; third row: (e and f) S2 25.06; fourth row: (g and h) platinum V.EU 25.06. The left column shows the images with the circular boxes indicating concentric abrasion marks at ×150; the right column shows the concentric abrasion marks at ×1000; and the skewed dimples near the center of rotation are typical features of torsional failure

depth of the helical canal, number and angle of cutting blades, and interlaminar distance) between the instruments justify the present results.[16,19]

Regarding cyclic and torsional fatigue resistance, notable differences were observed among the groups, leading to the rejection of the second null hypothesis. The mechanical properties of NiTi instruments can be influenced by cross-section, core diameter, tip diameter, and NiTi alloy heat treatment.[4,5] The mechanical behavior of instruments during the preparation of curved and/or atresic root canals must be confirmed by Micro-CT.[9] Although Silva *et al*.[4] and Jeong *et al*.[20] evaluated the mechanical properties of flat instruments compared to S-section instruments with identical heat treatments as the sole variable, the present results should be interpreted by associating different designs and heat treatments utilized in the NiTi alloys of the instruments.

Although the symmetric S-section provided greater cyclic fatigue resistance than the flat section, our results demonstrated that rotate instrument (symmetric S-section) exhibited lower time to fracture and fewer NCF than the platinum V.EU instrument (flat section).[4,16] In addition, the rotate system showed a fracture time similar to the S2 instrument (asymmetric S) and shorter than the spin rotary instrument (symmetric S). These findings suggest that despite uniform tip diameter and taper across all instruments, differences in NiTi alloy properties and manufacturer-recommended operating speeds likely influenced our study's outcomes. This reinforces the critical impact of cross-section design on the cyclic fatigue resistance of NiTi rotary instruments.[21]

A greater presence of martensitic and R-phase provided by heat treatments in NiTi alloys increases cyclic fatigue resistance.[4,12,22] Therefore, the result presented by the

rotate system is likely related to a NiTi alloy with more austenitic characteristics. These same factors also explain the differences observed among the S2 system, spin rotary system, and platinum V.EU system.

The higher activation speed of the instruments increases stress at the instrument's flexion point, reducing time to fracture.[23] Conversely, a higher speed results in more cycles per second for a given fracture activation time compared to an instrument operating at a lower speed.[23] Therefore, instruments activated at higher speeds should have shown less cyclic fatigue resistance.[4,20] However, the S2 system and spin rotary system exhibited longer fracture times, suggesting that the NiTi alloy had a more significant impact than speed in this study. Although flat cross-section instruments exhibit a lower maximum fracture force than those with a symmetric S-section, our results revealed that the rotate system exhibited significantly lower torque and greater angular deflection than the other instruments. Furthermore, there was no statistical difference among spin rotary system, S2 system, and the platinum V.EU system. This discrepancy is likely due to variations in instrument flexibility resulting from different thermal treatments and core diameters among the instruments.[9] The rotate system likely has a smaller core diameter, contributing to reduced fracture force and deformation capacity, despite featuring a NiTi alloy with more austenitic characteristics, thus explaining its torsional results. The absence of significant differences among the other groups can also be attributed to the combination of these factors discussed in the cyclic fatigue results.

This *in vitro* study presents certain limitations. The experimental setup, utilizing artificial canals and mandibular incisors, may not fully replicate the complex anatomical and physiological conditions encountered in a clinical setting, such as variations in root canal morphology, temperature fluctuations, and the presence of saliva or tissue fluids.

To expand upon these findings, future research could consider conducting *in vivo* studies to validate these *in vitro* observations under more realistic clinical conditions; performing differential scanning calorimetry to precisely characterize the crystallographic phases and transformation temperatures of the NiTi alloys used in these instruments, as suggested by the observed differences in mechanical properties.

CONCLUSION

Within the limitations of this study, the cross-sectional design of the tested systems did not influence the presence of the smear layer on dentin walls in flattened canals. The instruments exhibited significantly different mechanical properties, suggesting that heat treatments and core diameters had a more significant impact than cross-sectional designs.

Contribution Details

Conceptualization: João Pedro Tadano; Murilo Priori Alcalde; Ana Grasiela Limoeiro; Raimundo Sales Oliveira Neto; Methodology: João Pedro Tadano; Paula Tereza Galvao; Gulherme Ferreira da Silva; Formal analysis and investigation: Marco Antonio Hungaro Duarte; Writing – original draft preparation: João Pedro Tadano; Murilo Priori Alcalde; Ana Grasiela Limoeiro; Raimundo Sales Oliveira Neto; Pablo Amoroso-Silva; Writing: João Pedro Tadano; Murilo Priori Alcalde; Visualization: Ana Grasiela Limoeiro; Raimundo Sales Oliveira Neto; Pablo Amoroso-Silva; Supervision: Marco Antonio Hungaro Duarte.

Financial support and sponsorship

Nil.

Conflicts of interest

There are no conflicts of interest.

REFERENCES

1. Liu W, Wu B. Root canal surface strain and canal center transportation induced by 3 different nickel-titanium rotary instrument systems. J Endod 2016;42:299-303.
2. Wycoff RC, Berzins DW. An *in vitro* comparison of torsional stress properties of three different rotary nickel-titanium files with a similar cross-sectional design. J Endod 2012;38:1118-20.
3. Zupanc J, Vahdat-Pajouh N, Schäfer E. New thermomechanically treated NiTi alloys – A review. Int Endod J 2018;51:1088-103.
4. Silva EJ, Alcalde MP, Martins JN, Vieira VT, Vivan RR, Duarte MA, *et al.* To flat or not to flat? Exploring the impact of flat-side design on rotary instruments using a comprehensive multimethod investigation. Int Endod J 2023;56:1301-15.
5. Bürklein S, Zupanc L, Donnermeyer D, Tegtmeyer K, Schäfer E. Effect of core mass and alloy on cyclic fatigue resistance of different nickel-titanium endodontic instruments in matching artificial canals. Materials (Basel) 2021;14:5734.
6. Ayad OE, El Seoud MA, Kataia EM. Dynamic cyclic fatigue resistance of RACE EVO in S-shaped canal with different angles of access: An *in vitro* study. Saudi Endod J 2024;14:212-7.
7. Nagendrababu V, Murray PE, Ordinola-Zapata R, Peters OA, Rôças IN, Siqueira JF Jr., *et al.* PRILE 2021 guidelines for reporting laboratory studies in endodontology: A consensus-based development. Int Endod J 2021;54:1482-90.
8. Plotino G, Özyürek T, Grande NM, Gündoğar M. Influence of size and taper of basic root canal preparation on root canal cleanliness: A scanning electron microscopy study. Int Endod J 2019;52:343-51.
9. Weissheimer T, Duarte MA, Só MV, da Rosa RA, Espinosa MK, Vivan RR, *et al.* Evaluation of cyclic and torsional fatigue resistance of several heat-treated reciprocating nickel-titanium instruments. Aust Endod J 2023;49:524-9.
10. Alcalde MP, Tanomaru-Filho M, Bramante CM, Duarte MA, Guerreiro-Tanomaru JM, Camilo-Pinto J, *et al.* Cyclic and torsional fatigue resistance of reciprocating single files manufactured by different

nickel-titanium alloys. J Endod 2017;43:1186-91.
11. Furlan RD, Alcalde MP, Duarte MA, Bramante CM, Piasecki L, Vivan RR. Cyclic and torsional fatigue resistance of seven rotary systems. Iran Endod J 2021;16:78-84.
12. Alcalde MP, Duarte MA, Bramante CM, de Vasconselos BC, Tanomaru-Filho M, Guerreiro-Tanomaru JM, *et al*. Cyclic fatigue and torsional strength of three different thermally treated reciprocating nickel-titanium instruments. Clin Oral Investig 2018;22:1865-71.
13. Gambarini G, Miccoli G, Seracchiani M, Khrenova T, Donfrancesco O, D'Angelo M, *et al*. Role of the flat-designed surface in improving the cyclic fatigue resistance of endodontic NiTi rotary instruments. Materials (Basel) 2019;12:2523.
14. De-Deus G, Simões-Carvalho M, Belladonna FG, Cavalcante DM, Portugal LS, Prado CG, *et al*. Arrowhead design ultrasonic tip as a supplementary tool for canal debridement. Int Endod J 2020;53:410-20.
15. Alakshar A, Saleh AR, Gorduysus MO. Debris and smear layer removal from oval root canals comparing XP-endo finisher, EndoActivator, and manual irrigation: A SEM evaluation. Eur J Dent 2020;14:626-33.
16. Ashraf H, Zargar N, Zandi B, Azizi A, Amiri M. The evaluation of debris and smear layer generated by three rotary instruments neo NiTi, 2Shape and Revo_S: An *ex-vivo* scanning electron microscopic study. Iran Endod J 2023;18:96-103.
17. Poggio C, Dagna A, Chiesa M, Scribante A, Beltrami R, Colombo M. Effects of NiTi rotary and reciprocating instruments on debris and smear layer scores: An SEM evaluation. J Appl Biomater Funct Mater 2014;12:256-62.
18. Liu Y, Chen M, Tang W, Liu C, Du M. Comparison of five single-file systems in the preparation of severely curved root canals: An *ex vivo* study. BMC Oral Health 2022;22:649.
19. Liang Y, Yue L. Evolution and development: Engine-driven endodontic rotary nickel-titanium instruments. Int J Oral Sci 2022;14:12.
20. Jeong HY, Ha JH, Sigurdsson A, Peters OA, Kim HC, Kwak SW. Effects of side flattening on torsional and cyclic fracture resistance of nickel-titanium file. J Endod 2024;50:1011-6.
21. Di Nardo D, Gambarini G, Seracchiani M, Mazzoni A, Zanza A, Giudice A, *et al*. Influence of different cross-section on cyclic fatigue resistance of two nickel-titanium rotary instruments with same heat treatment: An *in vitro* study. Saudi Endod J 2020;10:221-5.
22. Campos GO, Fontana CE, Vieira VT, Elias CN, de Martin AS, Bueno CE. Influence of heat treatment of nickel-titanium instruments on cyclic fatigue resistance in simulated curved canals. Eur J Dent 2023;17:472-7.
23. Lopes HP, Ferreira AA, Elias CN, Moreira EJ, de Oliveira JC, Siqueira JF Jr. Influence of rotational speed on the cyclic fatigue of rotary nickel-titanium endodontic instruments. J Endod 2009;35:1013-6.